Rheology of Imidazolium-Based Ionic Liquids with Aromatic Functionality

ARTICLE *in* THE JOURNAL OF PHYSICAL CHEMISTRY B · JULY 2015

Impact Factor: 3.3 · DOI: 10.1021/acs.jpcb.5b06163 · Source: PubMed

2 AUTHORS:

Ran Tao

National Institute of Standards and Technology

6 PUBLICATIONS **14** CITATIONS

SEE PROFILE

Sindee L Simon

Texas Tech University

157 PUBLICATIONS **2,641** CITATIONS

SEE PROFILE

THE JOURNAL OF PHYSICAL CHEMISTRY B

Article

pubs.acs.org/JPCB

Rheology of Imidazolium-Based Ionic Liquids with Aromatic Functionality

Ran Tao and Sindee L. Simon*

Department of Chemical Engineering, Texas Tech University, Lubbock, Texas 79409, United States

ABSTRACT: A series of imidazolium-based ionic liquids with cyclic and aromatic groups and a bis[(trifluoromethane)sulfonyl]amide anion were characterized using dynamic and steady shear rheology in a wide temperature range. The cations investigated include 1-(cyclohexylmethyl)-3-methylimidazolium ($[CyhmC_1im]^+$), 1-benzyl-3-methylimidazolium ($[BnzC_1im]^+$), 1,3-dibenzylimidazolium ($[(Bnz)_2im]^+$), and 1-(2-naphthylmethyl)-3-methylimidazolium ($[NapmC_1im]^+$). Rheological properties are reported from terminal flow to the glassy state. All ionic liquids show very similar flow behavior with a glassy modulus approaching 1 GPa. The temperature dependences of the shift factors used for time−temperature superposition and the viscosity both follow the same VFT or WLF relationship, and the dynamic fragility at T_g ranges from 117 to 130 for the aromatic ionic liquids investigated, considerably more fragile, in the Angell sense, than the aliphatic analogs. Additionally, an anomalous aging effect in the dynamic viscosity response (i.e., a maximum observed at intermediate frequencies) was found using a strain-controlled rheometer but not using a stress-controlled rheometer.

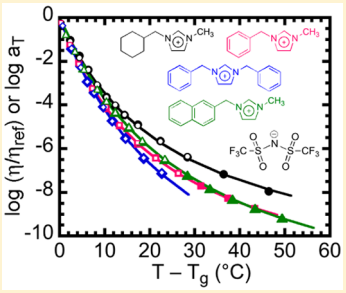

INTRODUCTION

Ionic liquids are a class of materials that possess attractive properties, including negligible vapor pressure, high ionic conductivity and thermal stability, good solvation ability and, generally, low rates of crystallization and good glass-forming ability. The great number of possible cation−anion combinations allows for tailoring ionic liquids with specific properties, and this has led to their being called "designer" solvents.[1] However, rational design of ionic liquids requires improved understanding of their structure−property relationships.

Thus far, a variety of techniques have been employed to study the relaxation dynamics of ionic liquids at temperatures approaching the glass transition temperature (T_g), including dielectric spectroscopy,[2−10] light scattering,[2,9] neutron scattering,[7,11] nuclear magnetic resonance (NMR) spectroscopy,[12,13] rheology,[3,7,14,15] Raman spectroscopy,[16,17] fluorescence recovery after photobleaching (FRAP),[18] and differential scanning calorimetry.[10,19−22] Many other temperature-dependent experiments have also been carried out in the supercooled liquid state, including viscosity measurements[22−30] and conductivity measurements.[22,27−31] A common observation in glass-forming liquids is that the temperature dependence of viscosity or relaxation time follows the Vogel−Fulcher−Tamman (VFT)[32−34] or Williams−Landel−Ferry (WLF) relationship,[35] from which the fragility index[36] m can also be obtained.

Among a variety of ionic liquids, n-alkyl substituted imidazolium cation-based ionic liquids are the most studied in the literature. While extensive investigations focus on the variation of the substituted alkyl chain length, much less attention has been paid to examine the effect of aromaticity on properties. In a previous study,[37] we established structure−property relationships for T_g, specific volume, and decomposition temperatures in imidazolium-based ionic liquids having cyclic and aromatic substituents on the cation and the same bis[(trifluoromethane)sulfonyl]amide ($[NTf_2]^-$) anion. In the present work, we perform shear rheology on the same four ionic liquids, namely, 1-(cyclohexylmethyl)-3-methylimidazolium ($[CyhmC_1im]^+$), 1-benzyl-3-methylimidazolium ($[BnzC_1im]^+$), 1,3-dibenzylimidazolium ($[(Bnz)_2im]^+$), and 1-(2-naphthylmethyl)-3-methylimidazolium ($[NapmC_1im]^+$) cations paired with a fixed anion $[NTf_2]^-$. Both dynamic and steady shear experiments are conducted, from which the temperature dependence of the reduced relaxation time and the viscosity are examined, and the dynamic fragility of each material is calculated.

EXPERIMENTAL SECTION

Materials. The synthesis of the ionic liquids has been described previously.[37,38] The structures and abbreviations of ionic liquids are shown in Figure 1. After synthesis, the samples were kept in tightly sealed vials and stored in an argon-filled glovebox or a desiccator. Prior to measurement, the ionic liquids were dried under vacuum at 50 °C for at least 24 h. The water content of the samples was determined to be less than 80 ppm by Karl Fischer titration using a Mettler-Toledo DL36 coulometer. When in use, the ionic liquids were constantly under a nitrogen atmosphere to minimize adventitious water absorption. After the rheological measurement, the water content of selected samples was measured to be less than 150 ppm. Such low water content is expected to have a negligible effect on the results.[39] The glass transition temperatures of the ionic liquids were measured by differential scanning calorimetry (DSC) on heating at 10 K/min from −120 to 40 °C after cooling from 40 to −120 °C at the same

Received: June 27, 2015
Published: July 31, 2015

DOI: 10.1021/acs.jpcb.5b06163
J. Phys. Chem. B 2015, 119, 11953−11959

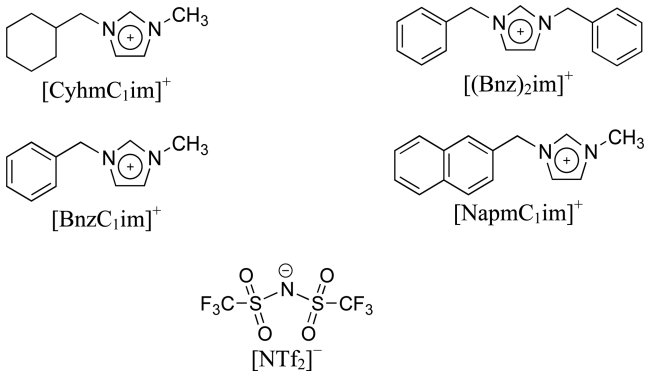

Figure 1. Structures of imidazolium-based cations $[CyhmC_1im]^+$, $[BnzC_1im]^+$, $[(Bnz)_2im]^+$, and $[NapmC_1im]^+$ paired with the $[NTf_2]^-$ anion.

rate. The DSC limiting fictive temperature (T_f') is taken to be T_g since T_f' measured on heating after cooling at a given rate approximates T_g measured on cooling at the same rate.[40] The DSC T_g values for the ionic liquids[37] are included in Table 1.

Rheological Measurements. Steady shear and dynamic oscillatory shear experiments were performed on the four ionic liquids using a Paar Physica MCR501 rheometer equipped with liquid nitrogen cooling system. Parallel plates of 8 and 25 mm diameter were used. The shear rates of measurement ranged from 10^{-5} to 10 s^{-1}, and the frequency ranged from 0.01 to 50 Hz. The testing temperatures were varied from the respective T_g to 50 °C above T_g for each ionic liquid. The strain was varied between 0.01% in the glassy state and 5% in the terminal region, all of which are in the linear viscoelastic range. For the runs made at lower temperatures ($T \leq T_g + 5$ °C), Struik's protocol[41] was applied with the testing time limited to one-tenth of the waiting time, in order to minimize physical aging effects. The gap between the plates was closely monitored and adjusted manually as the testing temperature was changed. All dynamic data are corrected for instrument compliance following the method by McKenna and co-workers.[42,43] The compliance of the total system using 8 and 25 mm diameter platens is 4.879×10^{-3} and 4.160×10^{-3} rad/Nm, respectively, measured by varying the deflection angle and recording the torque generated using platens glued together with zero gap with the glue applied to the outer edge of the platens. A phase angle check was performed using a dynamic frequency sweep from 0.1 to 100 rad/s on a 1000 cP Newtonian calibration fluid at room temperature using 25 mm parallel platens with a strain of 100%. The average phase angle is 89.85° ± 0.29° at all frequencies.

It is noted that Shamim and McKenna[15] found anomalous aging behavior for several alkylimidazolium ionic liquids. In the present study, we tried to reproduce their results on one of their samples, the high purity $[Bmim][BF_4]$, using both the Paar Physica, as well as the same instrument they used, namely the strain-controlled TA ARES rheometer. Dynamic frequency sweeps were performed from 100 to 0.001 rad/s at temperatures near, but above, T_g as a function of "aging" time. The first test was performed 30 min after reaching the test temperature to ensure temperature equilibration; subsequent tests were performed 30 min after the end of the preceding test. A steady shear sweep test was performed at the end of the series of dynamic tests. The same experimental procedure was followed and tested on the $[BnzC_1im][NTf_2]$ ionic liquid investigated herein using the strain-controlled ARES rheometer. It is noted that the temperatures of the two instruments differ with the Paar Physica temperature being ~0.9 K higher than that in the TA ARES based on the temperature-dependent viscosity values.

RESULTS

The dynamic storage (G') and loss (G'') moduli as a function of frequency (ω) for $[BnzC_1im][NTf_2]$ are shown in Figure 2

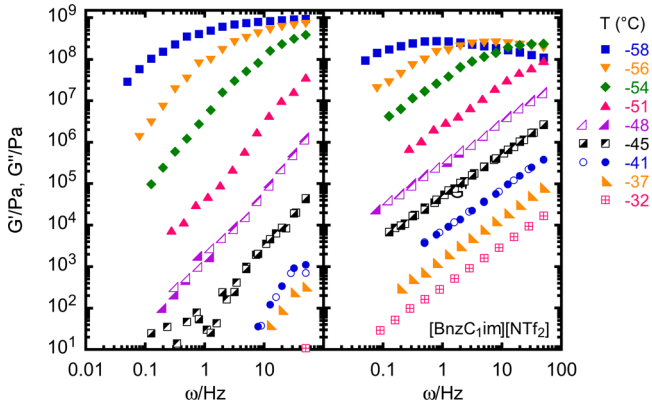

Figure 2. Storage modulus (G') and loss modulus (G'') as a function of frequency for the $[BnzC_1im][NTf_2]$ ionic liquid at the various temperatures indicated. View in color for best clarity.

at various temperatures from −58 to −32 °C. Repeat runs at several temperatures, shown by multiple symbols of the same color, indicate good reproducibility. The T_g of this ionic liquid is −58.3 °C as measured by DSC on heating at 10 K/min after cooling at the same rate.[37] Similar to the response of simple glass-forming materials, the ionic liquid shows a glassy response at low temperatures or high frequencies and flow behavior at high temperatures or low frequencies. The loss modulus goes through a maximum as the temperature decreases through glass transition. Because instrument compliance has a considerable impact on modulus, especially in the glassy regime,[42,43] corrections for instrument compliance have been made to the

Table 1. Glass Transition Temperature (T_g), WLF Constants (C_1 and C_2), Dynamic Fragility (m), and Apparent Activation Energy (E_g) at T_g for the Ionic Liquids Investigated

ionic liquid	$T_{g,DSC}$[a] (°C)	C_1	C_2 (K)	m	E_g (kJ/mol)	$T_{g\eta}$[b] (°C)
$[CyhmC_1im][NTf_2]$	−62.4	12.1	25.1	102	411	−63.6
$[BnzC_1im][NTf_2]$	−58.3	13.3	22.6	126	520	−58.9
$[(Bnz)_2im][NTf_2]$	−44.7	16.1	28.1	130	570	−44.0
$[NapmC_1im][NTf_2]$	−38.4	14.6	29.3	117	528	−38.0

[a] $T_{g,DSC}$ is measured on heating at 10 K/min from −120 to 40 °C after cooling from 40 to −120 °C at the same rate using differential scanning calorimetry. [b] $T_{g\eta}$ is defined as the temperature at which the viscosity equals 10^{10} Pa s.

DOI: 10.1021/acs.jpcb.5b06163
J. Phys. Chem. B 2015, 119, 11953−11959

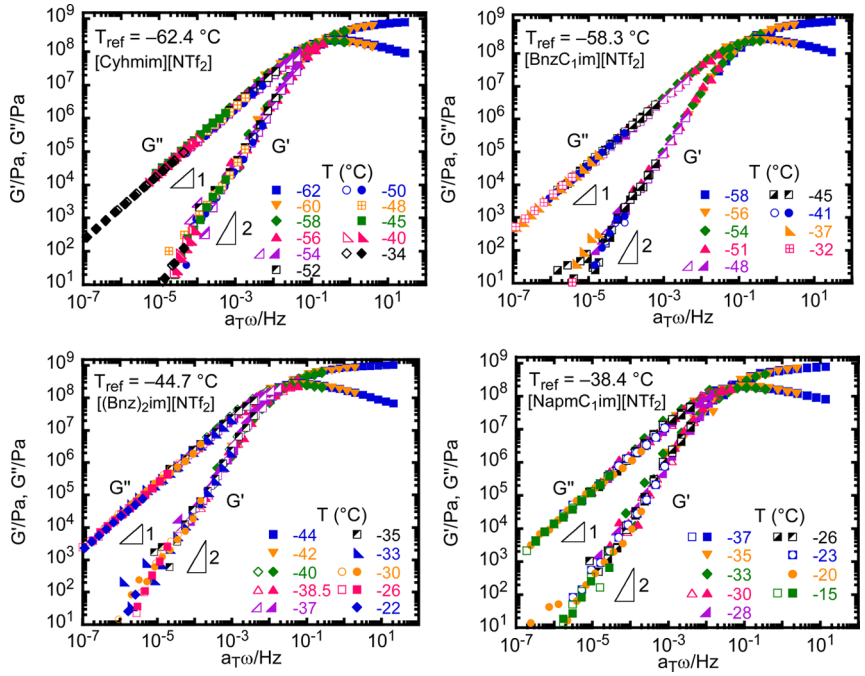

Figure 3. Reduced curves for G' and G'' for $[CyhmC_1im][NTf_2]$, $[BnzC_1im][NTf_2]$, $[(Bnz)_2im][NTf_2]$, and $[NapmC_1im][NTf_2]$ at T_{ref} = −62.4, −58.3, −44.7, and −38.4 °C, respectively. The expected slopes in the terminal region are indicated. View in color for best clarity.

G' and G'' data. The glassy modulus (G_g) value of ≈1 GPa is comparable with values found previously for other imidazolium-[14,15] and phosphonium-based ionic liquids.[14]

Time−temperature superposition of the $G'(\omega)$ and $G''(\omega)$ data is achieved applying horizontal shifts. No vertical shifts were applied for any of the ionic liquids in the present study. The reduced curves of G' and G'' are shown in Figure 3 for all of the samples investigated with reference temperatures indicated, which are approximately equal to their respective T_gs. The reduced curves for all of the ionic liquids are very similar: flow behavior is observed at low frequencies (where $dG'/d\omega = 2.0$ and $dG''/d\omega = 1.0$) and a glassy response is observed at high frequencies with a glassy storage modulus approaching 1 GPa. The large scatter in the terminal zone of the G' data at low frequencies is due to limitations in the phase angle measurement because as the phase angle δ approaches 90°, small errors in δ result in large errors in $G' = G^* \cos(\delta)$, where G^* is the complex shear modulus. Similarly large errors in the terminal G' data were observed by Pogodina et al.;[14] however, those authors interpreted their data to show a secondary relaxation by fitting G' data to a model with two distinct slopes (i.e., with a lower slope in the low-frequency region of 1 Pa < G' < 10^4 Pa). In the present work, we do not reach such an interpretation since deviations from the slope of 2.0 for G' data can be fully accounted for by errors in δ of 0.25°, which is within the error of the phase angle measurement.

A useful way to examine the dynamic rheological data is using the van Gurp−Palmen plot[44] as shown in Figure 4 for all four ionic liquids investigated, where the phase angle (δ) is plotted versus the complex shear modulus (|G*|). Note that the data presented in Figure 4 are from dynamic tests at different temperatures without any shifting, indicating that vertical shifts are not needed in constructing the reduced curves for G' and G'' in Figure 3, consistent with our findings. The shape of the van Gurp−Palmen plot is known to be very sensitive to the polydispersity, composition, and molecular architecture.[44−46]

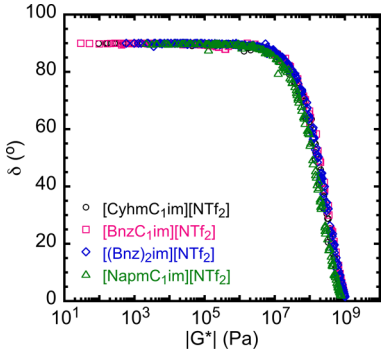

Figure 4. van Gurp−Palmen plot for the four ionic liquids investigated.

As is seen from the plot, the behavior is quite similar for all of the ionic liquids with different substituents on the imidazolium cation. The phase angle, $\delta = \tan^{-1}(G''/G')$, approaches 0° at high complex moduli of around 1 GPa, indicating a glass response and the corresponding glassy modulus of ≈1 GPa. As the modulus decreases, the phase angle increases, indicating the transition from an elastic response to a viscous response, and it reaches 90° at |G*| of 10^5 Pa, meaning that the flow behavior of a viscous liquid is attained. The van Gurp−Palmen plot clearly shows that the responses of the ionic liquids enter the terminal flow region and behave as viscous liquid as the modulus decreases to below 10^5 Pa. No evidence of a secondary relaxation is observed.

The steady state shear viscosity (η) as a function of shear rate ($\dot{\gamma}$) for the $[BnzC_1im][NTf_2]$ ionic liquid is shown in the same plot with the dynamic complex viscosity (η^*) as a function of frequency (ω) at various temperatures in Figure 5. In the limit of zero shear rate and zero frequency, values of η and η^* coincide at each temperature [i.e., $\lim_{\dot{\gamma}\to 0}\eta(\dot{\gamma}) = \lim_{\omega\to 0}\eta^*(\omega)$]. At temperatures close to T_g, the dynamic complex viscosity shows shear thinning behavior with increasing frequency. The

DOI: 10.1021/acs.jpcb.5b06163
J. Phys. Chem. B 2015, 119, 11953−11959

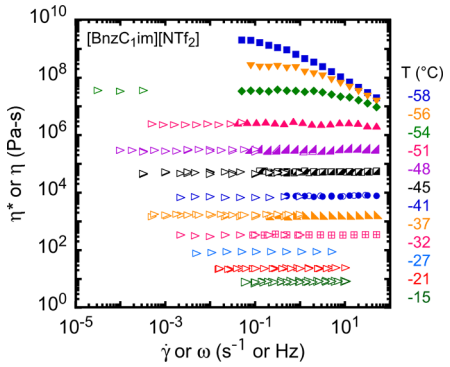

Figure 5. Double logarithmic plot of the steady state and the dynamic complex viscosity for $[BnzC_1im][NTf_2]$ at various temperatures ranging from −58 to −15 °C as a function of shear rate $\dot{\gamma}$ and ω, respectively. The steady shear viscosity is shown as open right-pointing triangles. The symbols for the dynamic complex viscosity are the same as in Figure 2. View in color for best clarity.

same behavior was found for the other three ionic liquids (data are not shown for brevity).

The temperature-dependent viscosity values are shown in Figure 6 for all of the ionic liquids, with values obtained from

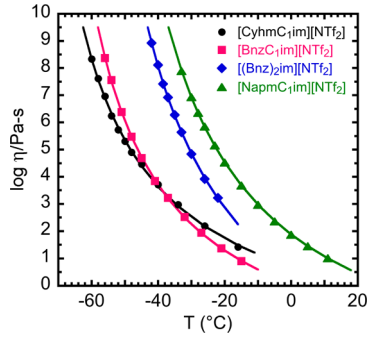

Figure 6. Steady state shear viscosity as a function of temperature for the four ionic liquids investigated. The solid lines are fits to the VFT equation.

the average of the limiting values at low $\dot{\gamma}$ and ω at each temperature. The temperature dependence is described by the Vogel−Fulcher−Tammann (VFT) equation:[32−34]

$$\eta(T) = \eta_0 \exp\left(\frac{B}{T - T_\infty}\right) \quad (1)$$

where η_0, T_∞, and B are material-dependent constants. The VFT equation is equivalent to the Williams−Landel−Ferry (WLF) equation:[35]

$$\log a_T = \log \frac{\eta}{\eta_{ref}} = -\frac{C_1(T - T_g)}{C_2 + (T - T_g)} \quad (2)$$

where C_1 and C_2 are material constants and η_{ref} is the viscosity at T_g. The VFT and WLF parameters are related to one another and to the dynamic fragility m and the apparent activation energy E_g at T_g:[47,48]

$$m = \frac{B/T_g}{\ln 10(1 - T_\infty/T_g)^2} = \frac{C_1 T_g}{C_2} \quad (3)$$

$$E_g = \frac{RB}{(1 - T_\infty/T_g)^2} = \ln 10 R \frac{C_1}{C_2} T_g^2 \quad (4)$$

where $C_2 = T_g - T_\infty$ and $B = \ln 10 C_1 C_2$.[47,49] The WLF values are reported in Table 1, as well as the values for m and E_g at the DSC T_g. The fragility index m is a measure of glass-forming ability and is used to classify glass-forming liquids as strong or fragile, with fragile liquids having large m values.[36] The dynamic fragilities range from 102 to 130 for this series of ionic liquids, which places them in the fragile category. The values are higher than those for alkylimidazolium cation-based ionic liquids which ranged from 38 to 97.[4,7,9,10,14,15,17,21] This is consistent with findings of Shirota et al.[50] who have also found that ionic liquids with aromatic moieties have high fragilities. In particular, based on their VFT parameters, the fragility index m is 130 for $[BnzC_1im][NTf_2]$ (compared to 126 for our work), and another benzyl-containing ionic liquid, 1-benzylpyridinium $[NTf_2]$, exhibits even higher fragility with m = 153.[50] Other ionic liquids with high fragilities reported in the literature include1-butyl-3-methylimidazolium bis(oxalato)borate with an m of 112,[27] 1-hexyl-3-methylimidazolium bromide with an m of 158,[4] 1-butyl-2,3-dimethylimidazolium tris(pentafluoroethyl)-trifluorophosphate with an m of 150,[26] and 1-ethyl-3-methylimidazolium dicyanamide with an m of 196.[30] The fragility of ionic liquids, which ranges from intermediate to extremely fragile,[27,30,47] is important because it correlates with the ionicity, which is a measure of the degree of ionic dissociation.[22,51] In addition, the roughly increasing correlations observed for our series of ionic liquids between fragility and T_g and between fragility and E_g are consistent with observations by Qin and McKenna for organic ionic liquids.[47]

The fragility of a glass-forming material depends on the choice of T_g.[52,53] The rheological T_g can be defined, according to Angell, as the temperature that corresponds to a viscosity of 10^{10} Pa s for glass-formers with T_g values below room temperature, in contrast to the commonly accepted value of 10^{12} Pa s for polymers.[27] As shown in Table 1, the rheological T_g is slightly different from T_g obtained by DSC, which is not unexpected since different techniques weigh the relaxation distribution differently.[40,54] Since the differences in T_g range from −1.2 to +0.7 K, the resulting changes in dynamic fragility [change in % $m \approx -2(\Delta T_g/C_2) \times 100\%$] are less than 10% for the four ionic liquids investigated, with m increasing at the rheological T_g if it is lower than the calorimetric T_g and vice versa if the rheological T_g is higher than the calorimetric T_g.

The incorporation of aromatic structure into an ionic liquid gives rise to an increase in fragility, and a similar pattern has been shown for small organic glass formers.[55] For example, in the T_g-scaled Arrhenius plot of viscosity, toluene was found to be more fragile than methylcyclohexane.[55] Leys et al.[4] studied fragility of a series of n-alkylimidazolium tetrafluoroborate with different alkyl chain length and found that the fragility depends on local interionic Coulombic forces between the cations and anions and is not strongly influenced by the alkyl substituents. In our case, the cyclic and aromatic substituents reduce molar volume compared to the alkyl counterpart (1-heptyl-3-methylimidazolium, denoted as C_7C_1)[37] (i.e., the molar volume follows the trend of $BnzC_1 < CyhmC_1 < NapmC_1 < C_7C_1$), which may result in a higher charge density on the cation and strengthen the electrostatic interaction. However, considering the impact of polarizability introduced by the π-electron clouds in the aromatic group, the influence of the interionic

DOI: 10.1021/acs.jpcb.5b06163
J. Phys. Chem. B 2015, 119, 11953−11959

Coulombic interactions and the induced charge van de Waals interactions on fragility is not obvious.

The temperature-dependence of the viscosity is compared to that of the shift factors obtained from reduction of the dynamic moduli data in Figure 7 as a function of $T - T_g$. The shift factor

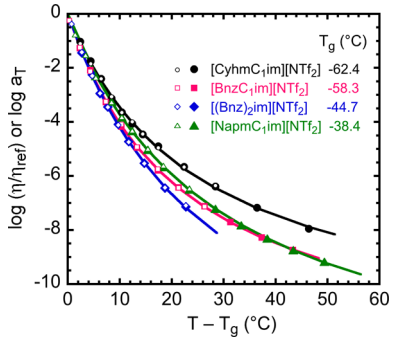

Figure 7. Reduced viscosity (filled symbols) and shift factors (open symbols) as a function of $T - T_g$ for the four ionic liquids investigated. The solid lines are fits to the VFT equation.

data can be described by the same VFT or WLF equation as reported for the viscosity, indicating that the underlying molecular motions for the α-relaxation and viscous flow are similar. The trend in fragility can also be observed for the data plotted versus $T - T_g$ in Figure 7: the less concave the curves, the higher the fragility of the ionic liquid.

DISCUSSION

An anomalous aging response was observed by Shamim and McKenna[15] for several alkylimidazolium ionic liquids, with the complex viscosity showing a maximum at intermediate frequencies during a first dynamic frequency sweep. The limiting dynamic viscosity and that at the maximum decreased in subsequent frequency scans and matched the steady shear viscosity when the sample was sufficiently "aged". Such behavior was not observed in the present study using the Paar Physica rheometer for the high purity 1-butyl-3-methylimidazolium tetrafluoroborate [Bmim][BF_4] used by Shamim and McKenna.[15] However, we have reproduced Shamim and McKenna's results on [Bmim][BF_4] using the instrument they used, namely the strain-controlled TA ARES rheometer. We also investigated aging effects for one of our ionic liquids and found a similar result. As shown in Figure 8, an anomalous aging response was also observed for [$BnzC_1$im][NTf_4] at two temperatures near T_g: the dynamic viscosity shows a maximum at intermediate frequencies for the first run and then decreases for subsequent runs toward the limiting low-frequency values. Note that the temperatures shown in Figure 8 were corrected according to the temperature-dependent viscosity values from the Paar Physica rheometer (Figure 6) since the temperature is slightly different for the two rheometers (with Paar Physica temperature being ~0.9 K higher than the TA ARES). The fact that the anomalous aging effect is observed by a strain-controlled rheometer and not by a stress-controlled rheometer is presumed to be due to their different working principles (i.e., a strain-controlled rheometer is equipped with separate motor and torque transducer and controls the strain directly, whereas a stress-controlled rheometer has a combined motor and transducer system and is subject to a relatively high inertia effect arising from the time lag between the strain acquisition and the stress imposition).

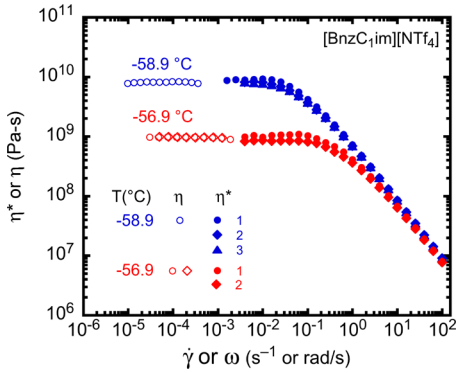

Figure 8. Double logarithmic plot of the steady state viscosity (η) and dynamic complex viscosity (η^*) of [$BnzC_1$im][NTf_2] measured using the TA ARES rheometer. Repeated tests were performed as shown by different symbols of the same color 30 min after the preceding test. The steady state viscosity tests (open symbols) were carried out after the dynamic tests. Note that the temperatures were corrected (−0.9 K) according to the temperature-dependent viscosity values (Figure 6) since the temperature is slightly higher for the Paar Physica than the ARES rheometer.

Zhang et al. have performed an in-depth study conducting nonlinear step strain experiments using both stress- and strain-controlled rheometers and observed different responses in the strain start-up transient period for the two types of instruments.[56] However, since rheological measurements presumed to be in the linear viscoelastic regime are expected to be independent of either instrument type, the observations in the present study and in Shamim and McKenna's work[15] are yet to be explained.

CONCLUSIONS

The rheological properties of a series of imidazolium-based ionic liquids with cyclic and aromatic groups have been investigated. Reduced curves for the dynamic shear modulus were constructed using time−temperature superposition, and the responses of all ionic liquids are found to be similar and to transition from flow behavior at low frequencies to a glassy response at high frequencies with a glassy moduli approaching 1 GPa. Analysis using the van Gurp−Palmen plot confirms the rheological similarity of all of the ionic liquids. No evidence of a secondary relaxation is observed in the terminal flow region below 10^5 Pa. The temperature-dependent shift factors and the viscosity both follow the same Vogel−Fulcher−Tamman or Williams−Landel−Ferry relationship, from which the dynamic fragility is obtained for each ionic liquid. The results show that ionic liquids with aromatic groups are fragile liquids in the Angell sense, having fragilities ranging from 117 to 130, higher than those of their aliphatic analogs. Additionally, an anomalous aging effect for the dynamic viscosity response with a maximum observed at intermediate frequencies in the dynamic complex viscosity was found using a strain-controlled rheometer but not by a stress-controlled rheometer.

AUTHOR INFORMATION

Corresponding Author

*E-mail: sindee.simon@ttu.edu.

Notes

The authors declare no competing financial interest.

DOI: 10.1021/acs.jpcb.5b06163
J. Phys. Chem. B 2015, 119, 11953−11959

■ ACKNOWLEDGMENTS

The authors would like to thank Prof. Edward L. Quitevis for providing the ionic liquid samples and Prof. Gregory B. McKenna for helpful discussions. Funding from Texas Tech Horn Professorship is gratefully acknowledged.

■ REFERENCES

(1) Freemantle, M. Designer Solvents. *Chem. Eng. News* **1998**, *76*, 32−37.
(2) Rivera, A.; Brodin, A.; Pugachev, A.; Rossler, E. A. Orientational and Translational Dynamics in Room Temperature Ionic Liquids. *J. Chem. Phys.* **2007**, *126*, 114503.
(3) Iacob, C.; Sangoro, J. R.; Serghei, A.; Naumov, S.; Korth, Y.; Karger, J.; Friedrich, C.; Kremer, F. Charge Transport and Glassy Dynamics in Imidazole-Based Liquids. *J. Chem. Phys.* **2008**, *129*, 234511.
(4) Leys, J.; Wubbenhorst, M.; Preethy Menon, C.; Rajesh, R.; Thoen, J.; Glorieux, C.; Nockemann, P.; Thijs, B.; Binnemans, K.; Longuemart, S. Temperature Dependence of the Electrical Conductivity of Imidazolium Ionic Liquids. *J. Chem. Phys.* **2008**, *128*, 064509.
(5) Rivera-Calzada, A.; Kaminski, K.; Leon, C.; Paluch, M. Ion Dynamics under Pressure in an Ionic Liquid. *J. Phys. Chem. B* **2008**, *112*, 3110−3114.
(6) Jarosz, G.; Mierzwa, M.; Ziolo, J.; Paluch, M.; Shirota, H.; Ngai, K. L. Glass Transition Dynamics of Room-Temperature Ionic Liquid 1-Methyl-3-Trimethylsilylmethylimidazolium Tetrafluoroborate. *J. Phys. Chem. B* **2011**, *115*, 12709−12716.
(7) Russina, O.; Beiner, M.; Pappas, C.; Russina, M.; Arrighi, V.; Unruh, T.; Mullan, C. L.; Hardacre, C.; Triolo, A. Temperature Dependence of the Primary Relaxation in 1-Hexyl-3-methylimidazolium Bis{(trifluoromethyl)sulfonyl}imide. *J. Phys. Chem. B* **2009**, *113*, 8469−8474.
(8) Ito, N.; Huang, W.; Richert, R. Dynamics of a Supercooled Ionic Liquid Studied by Optical and Dielectric Spectroscopy. *J. Phys. Chem. B* **2006**, *110*, 4371−4377.
(9) Griffin, P.; Agapov, A. L.; Kisliuk, A.; Sun, X. G.; Dai, S.; Novikov, V. N.; Sokolov, A. P. Decoupling Charge Transport From the Structural Dynamics in Room Temperature Ionic Liquids. *J. Chem. Phys.* **2011**, *135*, 114509.
(10) Viciosa, M. T.; Diogo, H. P.; Ramos, J. J. M. The Ionic Liquid BmimBr: A Dielectric and Thermal Characterization. *RSC Adv.* **2013**, *3*, 5663−5672.
(11) Triolo, A.; Russina, O.; Arrighi, V.; Juranyi, F.; Janssen, S.; Gordon, C. M. Quasielastic Neutron Scattering Characterization of the Relaxation Processes in a Room Temperature Ionic Liquid. *J. Chem. Phys.* **2003**, *119*, 8549−8557.
(12) Endo, T.; Widgeon, S.; Yu, P.; Sen, S.; Nishikawa, K. Cation and Anion Dynamics in Supercooled and Glassy States of the Ionic Liquid 1-Butyl-3-Methylimidazolium Hexafluorophosphate: Results from ^{13}C, ^{31}P, and ^{19}F NMR Spectroscopy. *Phys. Rev. B: Condens. Matter Mater. Phys.* **2012**, *85*, 054307.
(13) Chung, S. H.; Lopato, R.; Greenbaum, S. G.; Shirota, H.; Castner, E. W.; Wishart, J. F. Nuclear Magnetic Resonance Study of the Dynamics of Imidazolium Ionic Liquids with $-CH_2Si(CH_3)_3$ vs $-CH_2C(CH_3)_3$ Substituents. *J. Phys. Chem. B* **2007**, *111*, 4885−4893.
(14) Pogodina, N. V.; Nowak, M.; Lauger, J.; Klein, C. O.; Wilhelm, M.; Friedrich, C. Molecular Dynamics of Ionic Liquids as Probed by Rheology. *J. Rheol.* **2011**, *55*, 241−256.
(15) Shamim, N.; McKenna, G. B. Glass Dynamics and Anomalous Aging in a Family of Ionic Liquids above the Glass Transition Temperature. *J. Phys. Chem. B* **2010**, *114*, 15742−15752.
(16) Ribeiro, M. C. C. Correlation between Quasielastic Raman Scattering and Configurational Entropy in an Ionic Liquid. *J. Phys. Chem. B* **2007**, *111*, 5008−5015.
(17) Ribeiro, M. C. C. Low-Frequency Raman Spectra and Fragility of Imidazolium Ionic Liquids. *J. Chem. Phys.* **2010**, *133*, 024503.
(18) Bardak, F.; Rajian, J. R.; Son, P.; Quitevis, E. L. Heterogeneous Dynamics in Ionic Liquids at the Glass Transition: Fluorescence Recovery after Photobleaching Measurements of Probe Rotational Motion from $T_g - 6$ K to $T_g + 4$ K. *J. Non-Cryst. Solids* **2015**, *407*, 324−332.
(19) Yamamuro, O.; Minamimoto, Y.; Inamura, Y.; Hayashi, S.; Hamaguchi, H. Heat Capacity and Glass Transition of an Ionic Liquid 1-Butyl-3-Methylimidazolium Chloride. *Chem. Phys. Lett.* **2006**, *423*, 371−375.
(20) Shimizu, Y.; Ohte, Y.; Yamamura, Y.; Saito, K.; Atake, T. Low-Temperature Heat Capacity of Room-Temperature Ionic Liquid, 1-Hexyl-3-methylimidazolium Bis(trifluoromethylsulfonyl)imide. *J. Phys. Chem. B* **2006**, *110*, 13970−13975.
(21) Diogo, H. P.; Pinto, S. S.; Moura Ramos, J. J. Slow Molecular Mobility in the Amorphous Solid and the Metastable Liquid States of Three 1-Alkyl-3-Methylimidazolium Chlorides. *J. Mol. Liq.* **2013**, *178*, 142−148.
(22) Ueno, K.; Zhao, Z. F.; Watanabe, M.; Angell, C. A. Protic Ionic Liquids Based on Decahydroisoquinoline: Lost Superfragility and Ionicity-Fragility Correlation. *J. Phys. Chem. B* **2012**, *116*, 63−70.
(23) Zheng, W.; Mohammed, A.; Hines, L. G.; Xiao, D.; Martinez, O. J.; Bartsch, R. A.; Simon, S. L.; Russina, O.; Triolo, A.; Quitevis, E. L. Effect of Cation Symmetry on the Morphology and Physicochemical Properties of Imidazolium Ionic Liquids. *J. Phys. Chem. B* **2011**, *115*, 6572−6584.
(24) Moosavi, M.; Daneshvar, A. Investigation of the Rheological Properties of Two Imidazolium-Based Ionic Liquids. *J. Mol. Liq.* **2014**, *190*, 59−67.
(25) Burrell, G. L.; Dunlop, N. F.; Separovic, F. Non-Newtonian Viscous Shear Thinning in Ionic Liquids. *Soft Matter* **2010**, *6*, 2080−2086.
(26) Gacino, F. M.; Regueira, T.; Lugo, L.; Comunas, M. J. P.; Fernandez, J. Influence of Molecular Structure on Densities and Viscosities of Several Ionic Liquids. *J. Chem. Eng. Data* **2011**, *56*, 4984−4999.
(27) Xu, W.; Cooper, E. I.; Angell, C. A. Ionic Liquids: Ion Mobilities, Glass Temperatures, and Fragilities. *J. Phys. Chem. B* **2003**, *107*, 6170−6178.
(28) Tokuda, H.; Hayamizu, K.; Ishii, K.; Susan, M. A. B. H.; Watanabe, M. Physicochemical Properties and Structures of Room Temperature Ionic Liquids. 2. Variation of Alkyl Chain Length in Imidazolium Cation. *J. Phys. Chem. B* **2005**, *109*, 6103−6110.
(29) Smith, J. A.; Webber, G. B.; Warr, G. G.; Atkin, R. Rheology of Protic Ionic Liquids and Their Mixtures. *J. Phys. Chem. B* **2013**, *117*, 13930−13935.
(30) Schreiner, C.; Zugmann, S.; Hartl, R.; Gores, H. J. Temperature Dependence of Viscosity and Specific Conductivity of Fluoroborate-Based Ionic Liquids in Light of the Fractional Walden Rule and Angell's Fragility Concept. *J. Chem. Eng. Data* **2010**, *55*, 4372−4377.
(31) Capelo, S. B.; Méndez-Morales, T.; Carrete, J.; López Lago, E.; Vila, J.; Cabeza, O.; Rodríguez, J. R.; Turmine, M.; Varela, L. M. Effect of Temperature and Cationic Chain Length on the Physical Properties of Ammonium Nitrate-Based Protic Ionic Liquids. *J. Phys. Chem. B* **2012**, *116*, 11302−11312.
(32) Vogel, H. Das Temperaturabhängigkeit Gesetz der Viskosität von Flüssigkeiten. *Phys. Z.* **1921**, *22*, 645−646.
(33) Fulcher, G. S. Analysis of Recent Measurements of the Viscosity of Glasses. *J. Am. Ceram. Soc.* **1925**, *8*, 339−355.
(34) Tammann, G.; Hesse, W. Die Abhängigkeit der Viscosität von der Temperatur bie unterkühlten Flüssigkeiten. *Z. Anorg. Allg. Chem.* **1926**, *156*, 245−257.
(35) Williams, M. L.; Landel, R. F.; Ferry, J. D. The Temperature Dependence of Relaxation Mechanisms in Amorphous Polymers and Other Glass-Forming Liquids. *J. Am. Chem. Soc.* **1955**, *77*, 3701−3707.
(36) Angell, C. A. Relaxation in Liquids, Polymers and Plastic Crystals − Strong/Fragile Patterns and Problems. *J. Non-Cryst. Solids* **1991**, *131-133*, 13−31.
(37) Tao, R.; Tamas, G.; Xue, L. J.; Simon, S. L.; Quitevis, E. L. Thermophysical Properties of Imidazolium-Based Ionic Liquids: The

DOI: 10.1021/acs.jpcb.5b06163
J. Phys. Chem. B 2015, 119, 11953−11959

Effect of Aliphatic versus Aromatic Functionality. *J. Chem. Eng. Data* **2014**, *59*, 2717−2724.
(38) Dzyuba, S. V.; Bartsch, R. A. Influence of Structural Variations in 1-Alkyl(aralkyl)-3-Methylimidazolium Hexafluorophosphates and Bis(trifluoromethylsulfonyl)imides on Physical Properties of the Ionic Liquids. *ChemPhysChem* **2002**, *3*, 161−166.
(39) Seddon, K. R.; Stark, A.; Torres, M. J. Influence of Chloride, Water, and Organic Solvents on the Physical Properties of Ionic Liquids. *Pure Appl. Chem.* **2000**, *72*, 2275−2287.
(40) Badrinarayanan, P.; Zheng, W.; Li, Q. X.; Simon, S. L. The Glass Transition Temperature Versus the Fictive Temperature. *J. Non-Cryst. Solids* **2007**, *353*, 2603−2612.
(41) Struik, L. C. E. *Physical Aging in Amorphous Polymers and Other Materials*; Elsevier: Amsterdam, 1978.
(42) Schröter, K.; Hutcheson, S. A.; Shi, X.; Mandanici, A.; McKenna, G. B. Dynamic Shear Modulus of Glycerol: Corrections due to Instrument Compliance. *J. Chem. Phys.* **2006**, *125*, 214507.
(43) Hutcheson, S. A.; McKenna, G. B. The Measurement of Mechanical Properties of Glycerol, m-Toluidine, and Sucrose Benzoate under Consideration of Corrected Rheometer Compliance: An In-depth Study and Review. *J. Chem. Phys.* **2008**, *129*, 074502.
(44) van Gurp, M.; Palmen, J. Time−Temperature Superposition for Polymeric Blends. *Rheol. Bull.* **1998**, *67*, 5−8.
(45) Trinkle, S.; Friedrich, C. Van Gurp−Palmen−Plot: A Way to Characterize Polydispersity of Linear Polymers. *Rheol. Acta* **2001**, *40*, 322−328.
(46) Hu, M.; Xia, Y.; McKenna, G. B.; Kornfield, J. A.; Grubbs, R. H. Linear Rheological Response of a Series of Densely Branched Brush Polymers. *Macromolecules* **2011**, *44*, 6935−6943.
(47) Qin, Q.; McKenna, G. B. Correlation between Dynamic Fragility and Glass Transition Temperature for Different Classes of Glass Forming Liquids. *J. Non-Cryst. Solids* **2006**, *352*, 2977−2985.
(48) Simon, S. L.; Plazek, D. J.; Sobieski, J. W.; McGregor, E. T. Physical Aging of a Polyetherimide: Volume Recovery and Its Comparison to Creep and Enthalpy Measurements. *J. Polym. Sci., Part B: Polym. Phys.* **1997**, *35*, 929−936.
(49) Bernatz, K. M.; Echeverría, I.; Simon, S. L.; Plazek, D. J. Viscoelastic Properties of Amorphous Boron Trioxide. *J. Non-Cryst. Solids* **2001**, *289*, 9−16.
(50) Shirota, H.; Matsuzaki, H.; Ramati, S.; Wishart, J. F. Effects of Aromaticity in Cations and Their Functional Groups on the Low-Frequency Spectra and Physical Properties of Ionic Liquids. *J. Phys. Chem. B* **2015**, *119*, 9173−9187.
(51) Ueno, K.; Tokuda, H.; Watanabe, M. Ionicity in Ionic Liquids: Correlation with Ionic Structure and Physicochemical Properties. *Phys. Chem. Chem. Phys.* **2010**, *12*, 1649−1658.
(52) Zorn, R.; McKenna, G. B.; Willner, L.; Richter, D. Rheological Investigation of Polybutadienes Having Different Microstructures Over a Large Temperature Range. *Macromolecules* **1995**, *28*, 8552−8562.
(53) Koh, Y. P.; Grassia, L.; Simon, S. L. Structural Recovery of a Single Polystyrene Thin Film Using Nanocalorimetry to Extend the Aging Time and Temperature Range. *Thermochim. Acta* **2015**, *603*, 135−141.
(54) Tao, R.; Simon, S. L. Bulk and Shear Rheology of Silica/Polystyrene Nanocomposite: Reinforcement and Dynamics. *J. Polym. Sci., Part B: Polym. Phys.* **2015**, *53*, 621−632.
(55) Alba, C.; Busse, L. E.; List, D. J.; Angell, C. A. Thermodynamic Aspects of the Vitrification of Toluene, and Xylene Isomers, and the Fragility of Liquid Hydrocarbons. *J. Chem. Phys.* **1990**, *92*, 617−624.
(56) Zhang, H. G.; Lamnawar, K.; Maazouz, A.; Maia, J. Experimental Considerations on the Step Shear Strain in Polymer Melts: Sources of Error and Windows of Confidence. *Rheol. Acta* **2015**, *54*, 121−138.

DOI: 10.1021/acs.jpcb.5b06163
J. Phys. Chem. B 2015, 119, 11953−11959